Received: 29 September 2020 | Revised: 12 January 2021 | Accepted: 8 March 2021

DOI: 10.1002/joc.7089

RESEARCH ARTICLE

International Journal of Climatology RMetS

Effects of aerosols on cloud and precipitation in East-Asian drylands

Run Luo[1] | **Yuzhi Liu**[1,2] | **Qingzhe Zhu**[1] | **Yuhan Tang**[1] | **Tianbin Shao**[1]

[1]Key Laboratory for Semi-Arid Climate Change of the Ministry of Education, College of Atmospheric Sciences, Lanzhou University, Lanzhou, China

[2]Collaborative Innovation Center for Western Ecological Safety, Lanzhou University, Lanzhou, China

Correspondence
Yuzhi Liu, Key Laboratory for Semi-Arid Climate Change of the Ministry of Education, College of Atmospheric Sciences, Lanzhou University, Lanzhou 730000, China.
Email: liuyzh@lzu.edu.cn

Funding information
National Natural Science Foundation of China, Grant/Award Numbers: 41521004, 41991231, 91744311, 91937302; Strategic Priority Research Program of the Chinese Academy of Sciences, Grant/Award Number: XDA2006010301; Fundamental Research Funds for the Central Universities, Grant/Award Number: lzujbky-2020-kb02

Abstract

Extensive observational and numerical simulations have been performed to better characterize the role of aerosols in affecting the clouds and precipitation. However, due to the large uncertainties of aerosol property, the effect of aerosols on clouds and precipitation over the arid and semiarid region (briefly called 'drylands') of East Asia (EA) is still unclear. Basing on observations and model simulations from the Coupled Model Intercomparison Project Phase 5 (CMIP5), we investigated the aerosol's effects on the cloud properties and precipitation over the drylands of EA from 1850 to the present and projected forward to 2,300. It is found that, during 1850–2005, with the mean aerosol optical depth (AOD) over the drylands of EA increasing, the cloud droplet number concentration (CDNC) increases, while the cloud effective droplet radius (CEDR) decreases significantly at a rate of $-0.40\ \mu m \cdot century^{-1}$. Besides, the cloud water path (CWP) and precipitation show slightly increasing trends with the AOD increasing. Additionally, the effect of aerosols on cloud properties is saturated when the AODs reach 0.21 and 0.15 over the arid region (AR) and semiarid region (SR), respectively. According to the prediction for the period 2006–2300, the AOD and CDNC tend to decline over the drylands of EA, while the CWP, CEDR and precipitation show increasing trends. Particularly, the aerosol, clouds and precipitation indicate more significant changes over the SR in EA during 2006–2300. In future research, there is an urgent need to quantify the contribution of aerosol-cloud interaction to the precipitation change over the drylands of EA.

KEYWORDS

aerosol, arid and semiarid, cloud, East Asia, precipitation

1 | INTRODUCTION

Aerosols act a pivotal part in the hydrological cycle (Wang *et al*., 2010; Tao *et al*., 2012; Qi *et al*., 2013; Manaster *et al*., 2017; Liu *et al*., 2019a) and climate change (Houghton *et al*., 2001; Soden and Held, 2006; IPCC, 2007; Huang *et al*., 2008, 2017, 2018; Guan *et al*., 2015) by affecting the clouds and precipitation. Generally, aerosols have extremely complex climate effects classified into the direct effects (influencing the thermal balance by scattering and absorbing radiation), indirect effects (altering the radiation budget by affecting cloud properties) (Andreae, 1995; Charlson and Heintzenberg, 1995; Lohmann and Feichter, 2005;

Andreae and Rosenfeld, 2008; Bao *et al*., 2020). However, the processes of aerosol affecting the clouds and precipitation are complex, remaining poorly known (McComiskey and Feingold, 2012; Fan *et al*., 2016; Ma *et al*., 2020).

The arid and semiarid region (briefly called 'drylands') is considered as one of the most intensely affected regions by global climate change, in which the semiarid region (SR) has significantly warming and frequently extreme precipitation events in the past 100 years (Reynolds *et al*., 2007; Huang *et al*., 2012; Vallejo *et al*., 2012; Ryan and Elsner, 2016). In the drylands of East Asia (EA), especially in north China and northwest China, the water resources are extremely deficient (Sato, 2007; Huang *et al*., 2013; Liu *et al*., 2018, 2020a), and the drought has severely threatened the living environment, resulting in a series of environmental and social problems such as severe local water scarcity, ecological degradation and desertification (Huang *et al*., 2006; Wang and Chen, 2012; Liu *et al*., 2020b). Precipitation is one of the most essential processes to supply water resources in the drylands. In the process of precipitation formation, aerosol particles play a significant role in serving as condensation/ice nuclei for cloud droplet formation. Thus, studying the impact of aerosols on clouds and precipitation is of great importance and urgency to relieve the water resources shortage over the drylands of EA.

In recent years, the importance of aerosol emission, transport processes, and their effects on the clouds and precipitation in EA have been highlighted in many previous studies. Some studies focused on the aerosol's effects on cloud properties (Yan *et al*., 2015; Zhang *et al*., 2015), some focused on the effects of aerosols on precipitation (Zhao *et al*., 2006; Wang *et al*., 2011), and others paid more attention to the aerosol-cloud-precipitation interaction (Tao *et al*., 2012; Li *et al*., 2019). For the drylands of EA, Huang *et al*. (2014) systematically reviewed the numerous effects of dust aerosols on clouds and precipitation. Besides, there are some studies concentrated on other regions, such as southwest China (Fan *et al*., 2015), eastern China (Fan *et al*., 2012; Jiang *et al*., 2016; Guo *et al*., 2017) and Tibetan Plateau (Jiang *et al*., 2017; Jia *et al*., 2018; Liu *et al*., 2019b, 2019c; Hua *et al*., 2020) in EA. Due to the limitation of observation data, numerical simulation is an important method to study the impacts of aerosols on the cloud and precipitation. For example, Li *et al*. (2008) estimated the aerosol's effects on cloud formation and evolution using a two-moment bulk microphysical scheme, which has been applied in Weather Research and Forecasting (WRF) model. Jiang *et al*. (2013) evaluated the anthropogenic aerosol's impact on the clouds and precipitation in EA during the summer monsoon period using the NCAR Community Atmospheric Model version 5 (CAM5). Additionally, Qian *et al*. (2003) investigated the aerosol's properties and its climatic effects over China by comparing the observation and modelling results. Though the aerosol's effects on the cloud and precipitation have been examined in many previous studies (Fu *et al*., 2009; Li *et al*., 2011; Lee, 2012; Wang *et al*., 2013; Rosenfeld *et al*., 2014; Lee *et al*., 2015; Stjern and Kristjánsson, 2015; Li *et al*., 2017), a complete image of which presents over the whole drylands of EA and the discrepancy of which indicates over the arid region (AR) and SR is poorly known.

In this study, using the model results from Coupled Model Intercomparison Project Phase 5 (CMIP5) together with observational data, we investigated the relationship between the aerosol optical depth (AOD) and cloud properties including cloud water path (CWP), cloud droplet number concentration (CDNC), cloud effective droplet radius (CEDR) and further analysed the aerosol's effects on the clouds and precipitation during the future periods in drylands of EA.

2 | DATASETS

2.1 | CMIP5

CMIP5 can provide some evidence of aerosol-cloud-precipitation interactions for a long-term historical simulation and future projection. Considering both aerosol/cloud property parameters and experiments/scenarios included in the models, two models from CMIP5 are used, as listed in Table 1. Besides, these two models include the indirect effect of aerosols under four groups of experiments ('historical', 'historicalMisc', 'rcp45', and 'rcp85'). Here, for 'historicalMisc' experiment, only the anthropogenic aerosol forcing is involved. In the following, the 'historicalMisc' experiment is referred to as 'historicalAA'. Simultaneously, the monthly data 'od550aer' (Ambient Aerosol Optical Thickness at 550 nm), 'clwvi' (Condensed Water Path), 'cldncl' (Cloud Droplet Number Concentration of Cloud Tops), 'reffclwtop' (Cloud-Top Effective Droplet Radius) and 'pr' (Precipitation) are analysed, which is referred to as AOD, CWP, CDNC, CEDR and precipitation in the following. Basing on the output parameters of these two models, we use the data of CDNC and CEDR on the top of the liquid cloud. Here, the results of the model 'CSIRO-Mk3-6-0' have been interpolated to the horizontal resolution of 1.875° × 3.75°, getting the same resolution with the model 'IPSL-CM5A-LR'. The details of the experiments analysed in this study are described as follows (Taylor *et al*., 2012).

1. Experiment 'historical': The 20th century historical climate simulations are conducted with the best record of natural (mainly volcanic and solar) and

TABLE 1 Specific information of the datasets used in this study

Products	Key parameters	Spatial resolution
CRU (TS3.24)	Precipitation, potential evapotranspiration	0.5° × 0.5°
MODIS (MOD08_M3)	AOD, CWP, CEDR	1° × 1°
CMIP5 (historical, historicalMisc, rcp45, rcp85)	AOD, CWP, CDNC, CEDR, precipitation	CSIRO-Mk3-6-0 (1.875° × 1.875°) IPSL-CM5A-LR (1.875° × 3.75°)

Abbreviations: AOD, aerosol optical depth; CWP, cloud water path; CDNC, cloud droplet number concentration; CEDR, cloud effective droplet radius.

anthropogenic (e.g., aerosol emissions and land-use changes) climate forcing during the period 1850–2005.
2. Experiment 'historicalAA': Historical simulation but with anthropogenic aerosol forcing only.
3. Scenarios 'rcp45' and 'rcp85': Two future projection (2006–2,300) simulations under the scenario of rcp4.5 and rcp8.5 (referred to as 'representative concentration pathways'), which approximately results in a midrange radiative forcing of 4.5 $W \cdot m^{-2}$ and a high radiative forcing of 8.5 $W \cdot m^{-2}$ at the year 2,300, relative to pre-industrial conditions, respectively.

2.2 | CRU

The Climatic Research Unit (CRU), an institution related to natural and anthropogenic climate change, developed a lot of large-scale and high-resolution gridded climate datasets (CRU TS (Timeseries), CRU CY (Country) and CRU CL (Climatology)) with a horizontal resolution of 0.5° × 0.5°. In this study, we use the monthly mean potential evapotranspiration and precipitation data from 1901–2015 to define the AR and SR in EA. The precipitation data is also used to evaluate the precipitation derived from CMIP5 output under the 'historical' experiment.

2.3 | MODIS

In this study, the MOD08_M3 products from Moderate Resolution Imaging Spectroradiometer (MODIS) are used to evaluate the AOD, CWP and CEDR simulated by CMIP5 models. MOD08_M3, a level-3 MODIS global-gridded atmosphere monthly product collected from the Terra platform, contains monthly average values of atmospheric parameters, such as aerosol (e.g., aerosol optical depth and aerosol scattering angle), cloud (e.g., cloud fraction, cloud top pressure, cloud top temperature, cloud optical thickness and effective radius of both liquid water and ice clouds) properties, water vapour and atmosphere profile. The resolution of the monthly AOD, CWP and CEDR data used here is 1.0° × 1.0° during 2000–2005.

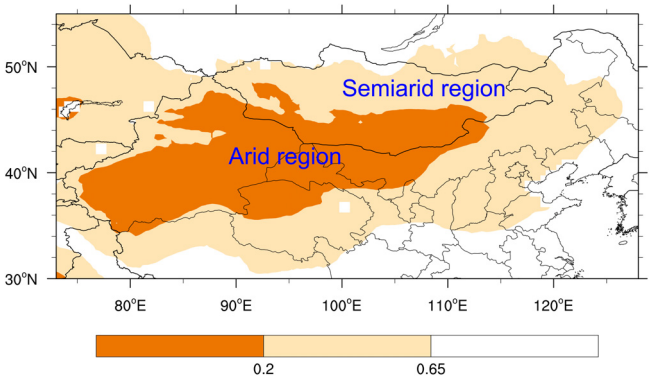

FIGURE 1 Distribution of the arid region (AR) and semiarid region (SR) in East Asia. Orange and yellow colours denote AR and SR, respectively [Colour figure can be viewed at wileyonlinelibrary.com]

Here, the details of this product are summarized in Table 1.

3 | RESULTS AND ANALYSES

3.1 | Aerosol, cloud and precipitation properties and their changes

This study focuses on the drylands where the aridity index (AI, defined as the ratio of precipitation and potential evapotranspiration) is less than 0.65, including AR with AI values of less than 0.2 and SR with AI ranging from 0.2 to 0.65. The drylands in EA is located between 31°N–52°N and 77°E–125°E, as shown in Figure 1. Before investigating the effects of aerosol on cloud property and precipitation derived from CMIP5 models, the model ability of simulating aerosol, cloud and precipitation properties are evaluated by the MODIS observations and CRU data during the overlapping period of 2000–2005.

Figure 2 shows the spatial distribution of annual mean AOD and CWP observed by MODIS product and simulated by CMIP5 models under the 'historical' experiment over the drylands of EA during 2000–2005. As shown in Figure 2, a comparison between MODIS product and CMIP5 simulations indicates a consistent spatial

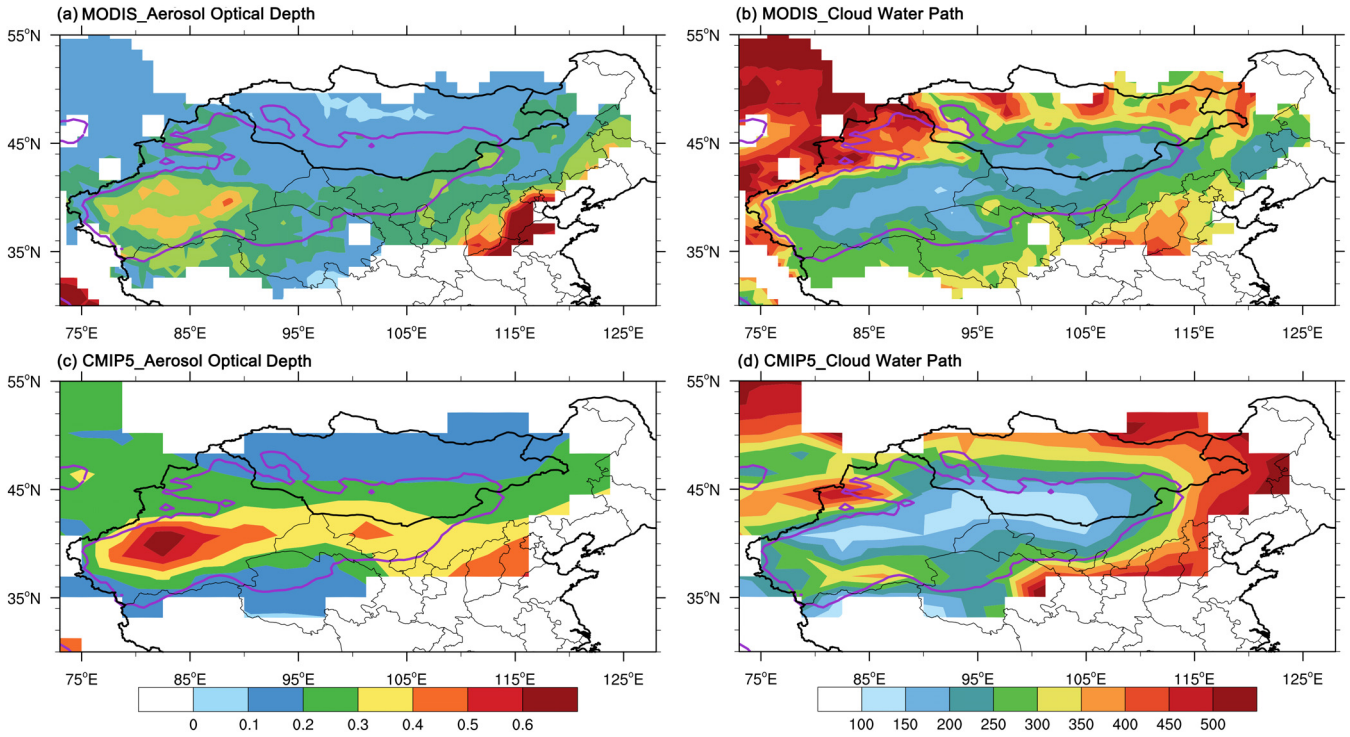

FIGURE 2 Distribution of AOD and CWP ($g \cdot m^{-2}$) derived from (a, b) MODIS product and (c, d) model simulations of CMIP5 under the 'historical' experiment over the drylands of EA during 2000–2005. The areas inside and outside the purple curve represent AR and SR, respectively [Colour figure can be viewed at wileyonlinelibrary.com]

TABLE 2 Annual mean and standard deviation of AOD, CWP, CEDR and precipitation over the drylands of EA during the period 2000–2005 (units: 1, $g \cdot m^{-2}$, μm, mm)

		East Asia		
Parameter	**Data**	**Total**	**Arid**	**Semiarid**
AOD	MODIS	0.24 (0.06)	0.25 (0.03)	0.23 (0.07)
	CMIP5	0.26 (0.04)	0.31 (0.05)	0.24 (0.04)
CWP	MODIS	303.86 (32.10)	236.85 (33.24)	340.89 (32.11)
	CMIP5	303.38 (40.99)	203.23 (25.24)	361.45 (44.36)
CEDR	MODIS	14.32 (0.21)	13.39 (0.34)	14.83 (0.23)
	CMIP5	4.19 (0.59)	4.07 (0.57)	4.27 (0.60)
Precipitation	CRU	248.69 (30.01)	107.36 (11.79)	327.73 (29.24)
	CMIP5	398.08 (54.52)	227.45 (49.97)	497.00 (42.03)

distribution. The AOD and CWP over the drylands of EA are basically below 0.6 and 500 $g \cdot m^{-2}$, respectively. The regional mean AODs derived from the MODIS and CMIP5 simulation during 2000–2005 over the drylands of EA are 0.24 and 0.26, respectively (Table 2). Based on the MODIS product, as listed in Table 2, the regional mean AODs over the AR (0.25) is larger than that over the SR (0.23) of EA. The average AODs obtained from model results over the AR and SR are slightly larger than those from MODIS, which are 0.31 and 0.24, respectively. Besides, the average CWPs derived from MODIS product and model simulation over the drylands of EA have nearly the same values of 303.86 $g \cdot m^{-2}$ and 303.38 $g \cdot m^{-2}$, respectively. Separately, the MODIS-observed regional mean CWPs over the AR and SR of EA are 236.85 $g \cdot m^{-2}$ and 340.89 $g \cdot m^{-2}$, respectively, which are underestimated and overestimated by CMIP5 models under the 'historical' experiment over the AR (203.23 $g \cdot m^{-2}$) and SR (361.45 $g \cdot m^{-2}$) of EA, respectively. Overall, during 2000–2005, the observed and estimated AOD and CWP indicate good consistency over the drylands of EA.

Besides, Figure 3 also indicates a good agreement (Figure 3a,c) in the spatial distributions of CEDR by MODIS observation and model simulation under the

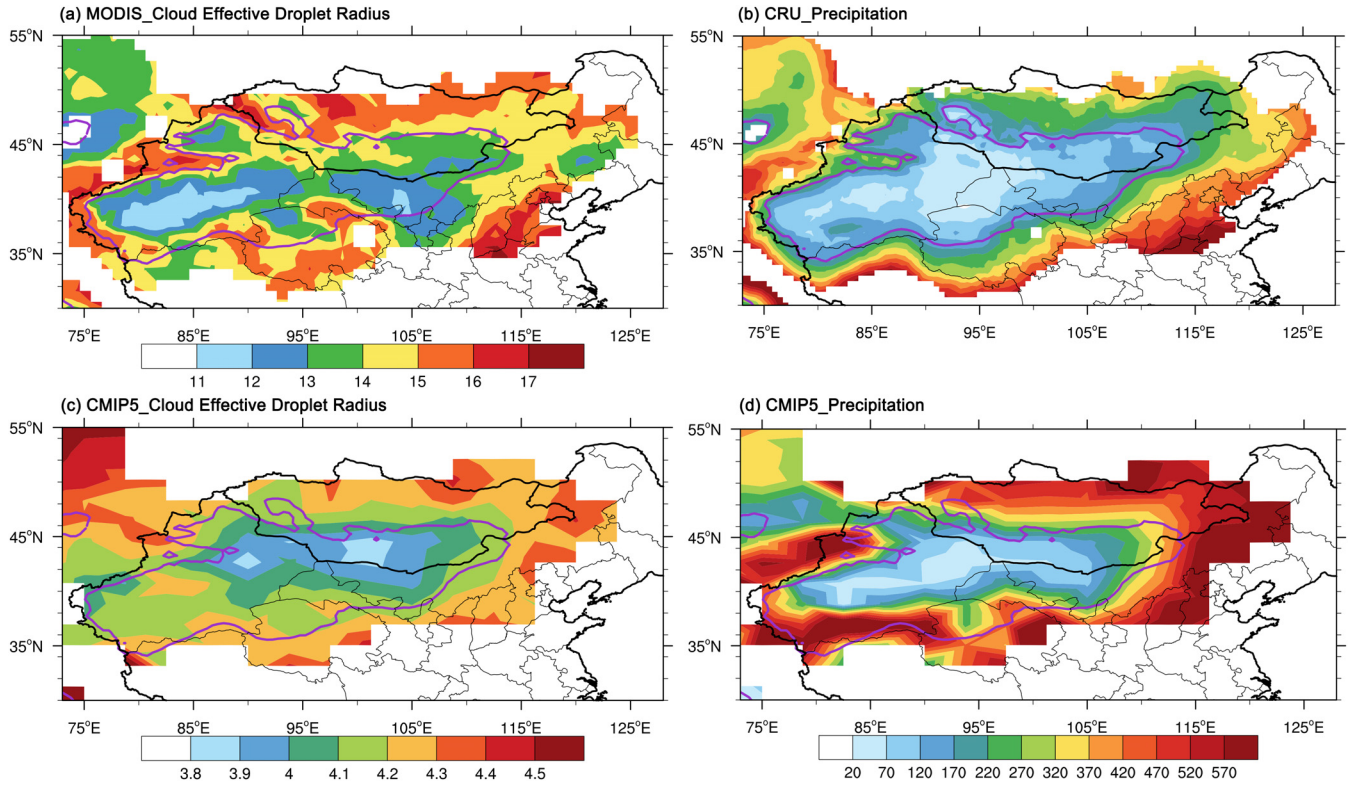

FIGURE 3 Distribution of CEDR (μm) and precipitation (mm) derived from (a) MODIS product, (b) CRU data and (c, d) CMIP5 model results under the 'historical' experiment over the drylands of EA during 2000–2005. The areas inside and outside the purple curve represent AR and SR, respectively [Colour figure can be viewed at wileyonlinelibrary.com]

'historical' experiment. The regional mean CEDRs derived from MODIS and CMIP5 results over the drylands of EA are 14.32 μm and 4.19 μm, respectively (Table 2). Additionally, according to the CMIP5 model results, the regional mean CEDRs over the AR and SR of EA are 4.07 μm and 4.27 μm, respectively, which are significantly lower than those derived from MODIS product (13.39 μm over the AR and 14.83 μm over the SR). Here, the significant difference may be induced by the data difference in getting the CEDR at the top of clouds in CMIP5 but in the whole cloud layers in MODIS measurements. Though such a difference exists, a reasonable range of CEDR simulated by CMIP5 models is affirmed. Similarly, there is an overall consistency in the spatial distribution of the precipitation between the CRU data and model simulations. The regional mean precipitations from CRU data and model simulation over the drylands of EA are 248.69 mm and 398.08 mm, respectively. And the observed precipitations over the AR and SR of EA are 107.36 mm and 327.73 mm (Table 2), respectively. On the whole, the CMIP5 models overestimate the precipitation under the 'historical' experiment (the values are 227.45 mm and 497.00 mm over the AR and SR, respectively). In general, although there is some bias in values of CMIP5 model simulations compared with observations, the simulated CWP, CEDR and precipitation are in reasonable agreement with the observations in spatial pattern and can be used to analyse the aerosol's effects on clouds and precipitation.

The distributions of AOD, CWP, CEDR and precipitation obtained from the CMIP5 results under the 'historical' experiment during 1850–2005 are nearly consistent with those from 2000–2005. Moreover, the spatial distributions of CDNC derived from the 'historical' experiment during 1850–2005 are similar to the distributions of CEDR over the drylands of EA. Here, the figures for the annual mean AOD, CWP, CDNC, CEDR and precipitation during 1850–2005 are omitted. Furthermore, the annual mean values of these parameters over the AR and SR of EA from 1850–2005 are listed in Table 3. Except for AOD, the annual mean CWP, CDNC, CEDR and precipitation values over the SR are higher than those over the AR. The annual mean AOD, CWP, CDNC, CEDR and precipitation over the AR are 0.27, 188.34 $g \cdot m^{-2}$, 0.10 mm^{-3}, 4.31 μm and 212.53 mm, respectively, and those over the SR are 0.15, 347.08 $g \cdot m^{-2}$, 0.11 mm^{-3}, 4.48 μm and 471.62 mm, respectively.

Basing on the 'historical' simulations by CMIP5 models, we analysed the time series of annual mean properties of aerosol, cloud and precipitation. Figure 4

TABLE 3 Annual variation of AOD, CWP, CDNC, CEDR, precipitation simulated by CMIP5 models over the drylands of EA during 1850–2005

	Arid		Semiarid	
Parameter	**Mean**	**Trend**	**Mean**	**Trend**
AOD	0.27	0.05[c]	0.15	0.08[c]
CWP	188.34	10.16[c]	347.08	12.18[c]
CDNC	0.10	0.04[c]	0.11	0.04[c]
CEDR	4.31	−0.41[c]	4.48	−0.37[c]
Precipitation	212.53	6.57[b]	471.62	5.28[a]

Note: Label [a], [b] and [c] indicate that the trends are significant above the 90%, 95% and 99% confidence level, respectively (units: century^{-1}, g·m^{-2} (g·m^{-2}·century^{-1}), mm^{-3} (mm^{-3}·century^{-1}), μm (μm·century^{-1}), mm (mm·century^{-1})).

presents the time series of annual mean anomalies of AOD, CWP, CDNC, CEDR and precipitation from model simulations of CMIP5 under the 'historical' experiments over the drylands of EA during 1850–2005. As shown in Figure 4, except for CWP and precipitation, the AOD, CDNC and CEDR indicate significant trends during 1850–2005, especially during the second half of the 20th century. Overall, during the period 1850–2005, the AOD and CDNC tend to increase significantly at rates of 0.07 century^{-1} and 0.04 mm^{-3}·century^{-1} over the drylands of EA, respectively. In contrast, the CEDR shows an incredible decreasing trend at a rate of −0.40 μm·century^{-1}. Compared with other parameters, the CWP and precipitation indicate slightly increasing trends at approximately 11.52 g·m^{-2}·century^{-1} and 5.80 mm·century^{-1} over the drylands of EA, respectively. All of those trends are significant at the 95% confidence level. Additionally, as listed in Table 3, the AODs over the AR and SR of EA tend to increase at rates of 0.05 century^{-1} and 0.08 century^{-1}, respectively. A more significant trend of CWP was found over the SR, in which the increasing trend with a significance above the 99% confidence level is 12.18 g·m^{-2}·century^{-1}. For the CDNC, there is a similar increasing trend at the rate of 0.04 mm^{-3}·century^{-1} over the AR and SR. Compared with AOD and CWP, the decrease in CEDR and an increase in precipitation over the AR are more significant than those over the SR. The CEDRs over the AR and SR of EA tend to decrease at rates of −0.41 μm·century^{-1} and -0.37 μm·century^{-1}, respectively. Besides, the precipitation shows increasing trends at rates of 6.57 mm·century^{-1} and 5.28 mm·century^{-1} over the AR and SR of EA, respectively, in which the significance confidence level is higher over the SR. In a word, compared with the changes in AOD and CWP over the AR with those over the SR of EA, the increases in the AOD and CWP are more intensively over the SR, while the trends of CEDR and precipitation are more significant over the AR.

On the whole, basing on CMIP5 model simulations over the drylands of EA for historical period from 1850–2005, it can be found that with the increasing of AOD, the CEDR decreases, however, the CDNC, CWP and precipitation increase. Furthermore, time evolutions of these parameters simulated by models under the 'historicalAA' experiment (including both direct and indirect effects) are presented in Figure 5. The AOD and CDNC tend to increase significantly at rates of 0.08 century^{-1} and 0.05 mm^{-3}·century^{-1} over the drylands of EA under the 'historicalAA' experiment, respectively. For the CEDR, a significantly decreasing trend at a rate of −0.47 μm·century^{-1} was found over there. Overall, the changes in AOD, CDNC and CEDR under the 'historicalAA' experiment are consistent with those under the 'historical' experiment. Compared with the CDNC and CEDR, the CWP (−6.66 g·m^{-2}·century^{-1}) and precipitation (−13.80 mm·century^{-1}) show slightly decreasing trends under the 'historicalAA' experiment during period 1850–2005, which are opposite to the changes under the 'historical' experiment.

3.2 | Aerosol-cloud-precipitation interaction

Combining the variations of aerosols, clouds and precipitation from the model simulations of CMIP5 under the 'historical' and 'historicalAA' experiments over the drylands in EA during 1850–2005, some significant relationship between aerosol, cloud and precipitation was found. In the following, a detailed analysis is performed. Figure 6 shows the spatial distributions of the correlation coefficient between annual mean AOD and CWP, CDNC, CEDR, precipitation simulated by CMIP5 models under the 'historical' experiment over the drylands of EA from 1850 to 2005. As shown in Figure 6a, a positive correlation with significance above the 90% confidence level can be found between the AOD and CWP in most areas of drylands in EA, especially in the north area of East-Asian drylands. Similarly, there is a high correlation coefficient about positive 0.8 between AOD and CDNC (Figure 6b). However, a negative correlation with coefficient about negative 0.8, with significance above the 90% confidence level, between annual mean AOD and CEDR is notable in the drylands of EA, as shown in Figure 6c. Besides, a regional difference is found in the relationship between AOD and precipitation, in which most of the areas located in the north portion of the East-Asian drylands show a positive correlation but most southern areas indicate a negative correlation. And most of the correlations

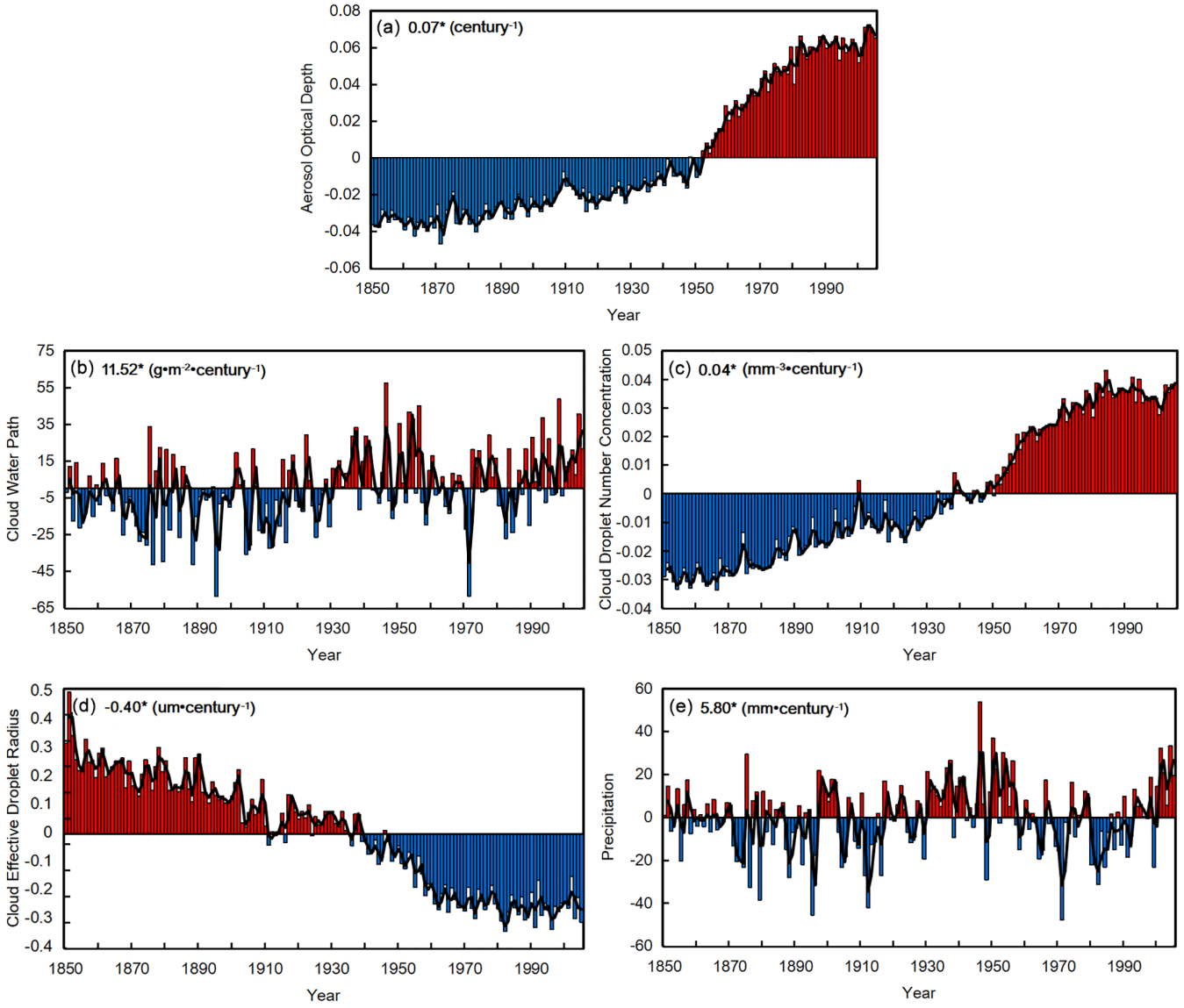

FIGURE 4 Time series of (a) AOD, (b) CWP, (c) CDNC, (d) CEDR, and (e) precipitation anomalies simulated by the models of CMIP5 under the 'historical' experiment over the drylands of EA during 1850–2005. Red and blue bars indicate positive and negative anomalies, respectively. Thick solid black line indicates a 3-year running average. The trends of each parameter are marked on the top left of (a)–(e), in which the asterisk denotes the trend is significant above the 95% confidence level [Colour figure can be viewed at wileyonlinelibrary.com]

over the northern areas have passed the significance test above the 90% confidence level.

Taking into account the uneven sample distribution influence on the relationship between aerosol, clouds and precipitation, the weight of each AOD bin in the total samples was considered. Figure 7 illustrates the percentage of sample numbers in different AOD bins out of the total samples in drylands of EA from 1850 to 2005. In the whole region of drylands in EA, with the 1873 valid samples, the AOD ranges from 0.05 to 0.40. The aerosols are mainly concentrated in the bins of AOD varying from 0.06 to 0.36 over the drylands of EA, and the peak percentage of all samples was found in the AOD bin of 0.10 with the value reaches 4.7%. To avoid the uneven sample distribution influence on the relationship fitting, we performed the following analyses for the AOD bins with a sample weight exceeding 1%.

Figure 8 shows the relationships between the CWP, CDNC, CEDR, precipitation and AOD in the drylands of EA. As presented in Figure 8a, with the AOD increasing from 0.06 to 0.21, the CWP increases significantly from 100.62 $g{\cdot}m^{-2}$ to 419.43 $g{\cdot}m^{-2}$. However, when the AOD is greater than 0.21, the CWP increases slightly and remains independent of changes in the AOD. Meanwhile, the CDNC is significantly dependent on the AOD and the linear slope between the CDNC and AOD is 0.16 mm^{-3}.

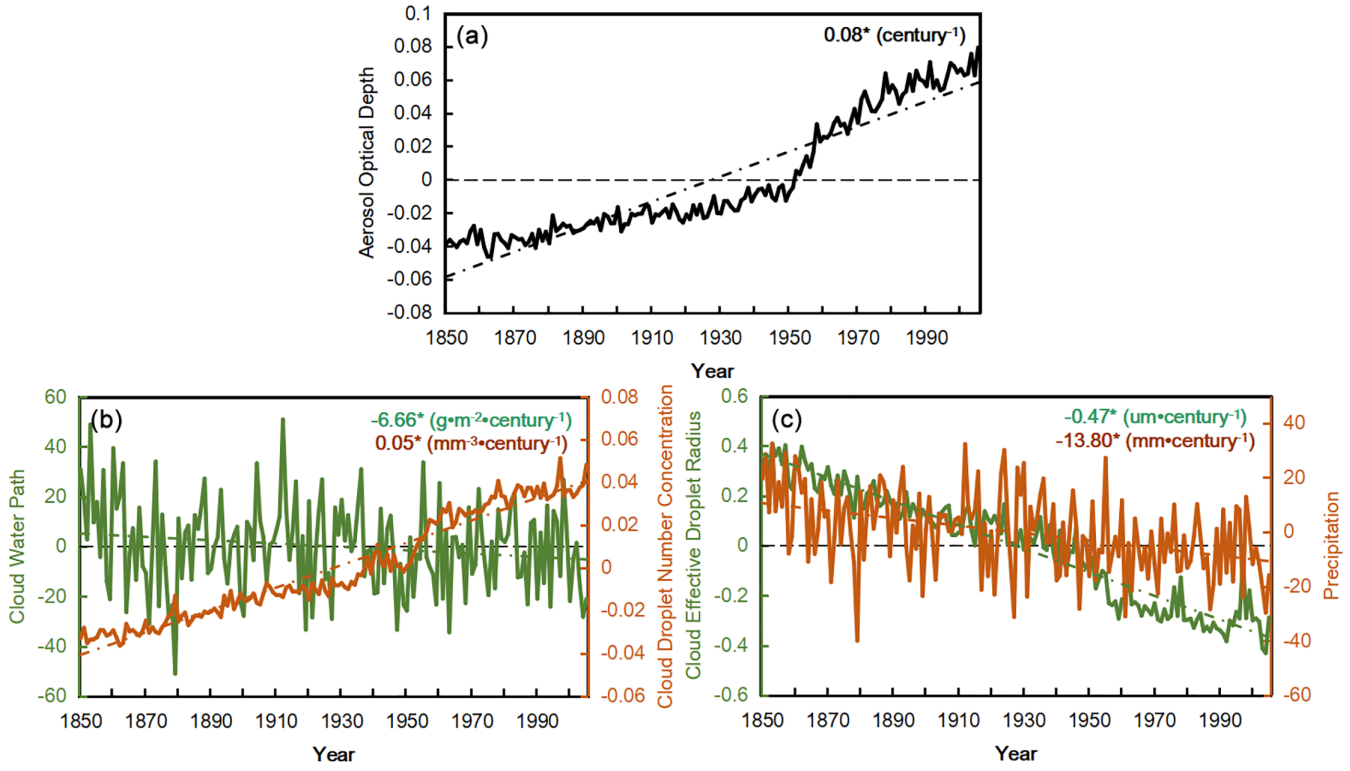

FIGURE 5 Time series of (a) AOD, (b) CWP and CDNC, (c) CEDR and precipitation anomalies from CMIP5 model results under the 'historicalAA' experiment over the drylands of EA during 1850–2005. The trends are marked on the top right of (a)–(c), in which the asterisk indicates the trend is significant above the 95% confidence level [Colour figure can be viewed at wileyonlinelibrary.com]

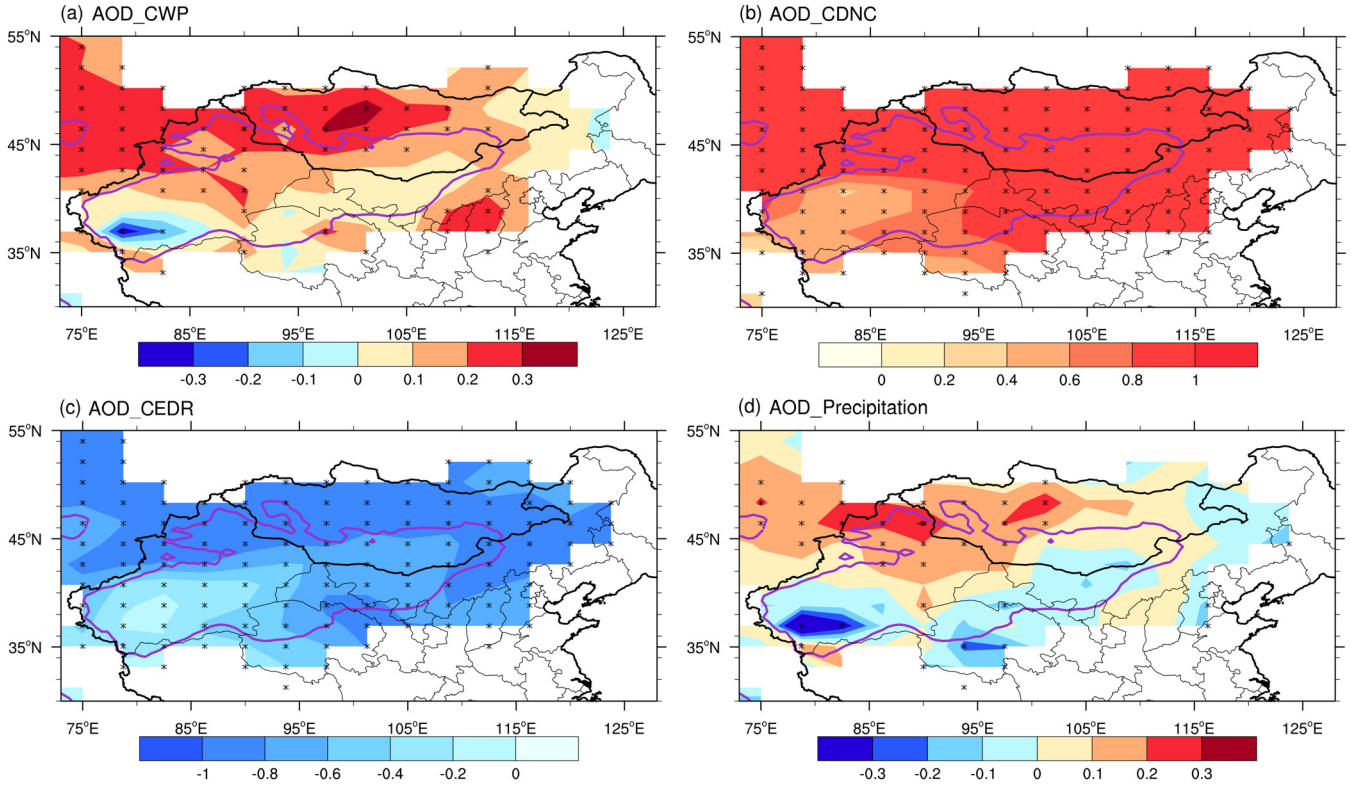

FIGURE 6 Spatial distribution of correlation coefficient between annual mean AOD and (a) CWP, (b) CDNC, (c) CEDR, (d) precipitation from model results under the 'historical' experiment over the drylands of EA during 1850–2005. The black asterisk indicates the correlation is significant above the 90% confidence level [Colour figure can be viewed at wileyonlinelibrary.com]

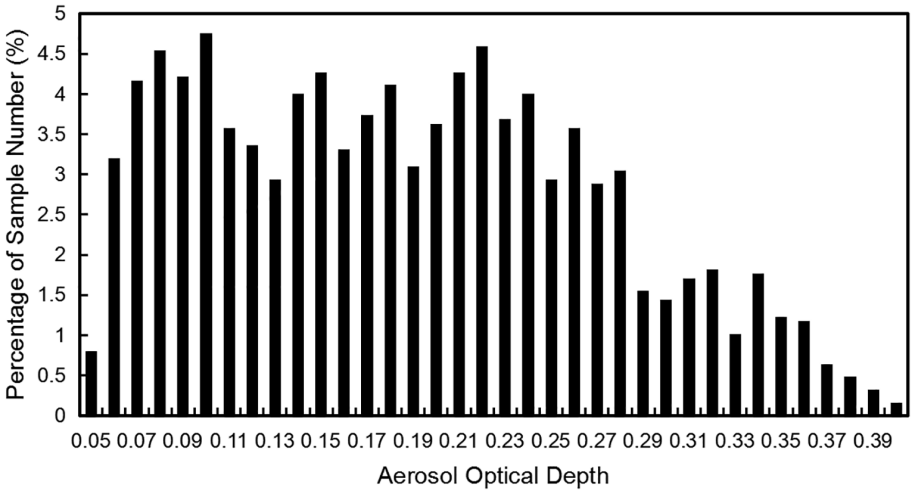

FIGURE 7 Percentage (%) of sample numbers in different AOD bins out of the total samples in the drylands of EA during 1850–2005

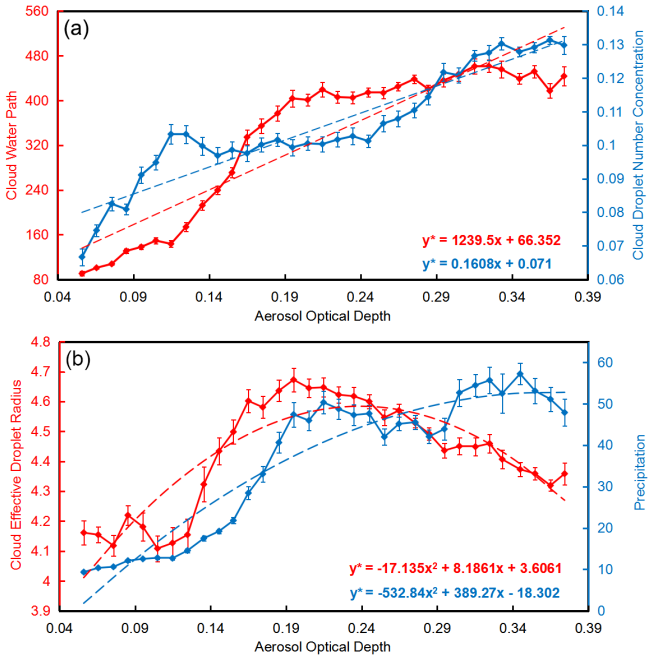

FIGURE 8 Monthly mean (a) CWP (red) and CDNC (blue), (b) CEDR (red) and precipitation (blue) for constant bins of AOD from CMIP5 simulations under the 'historical' experiment over the drylands of EA during 1850–2005. Error bar represents the confidence level of the mean value, which is calculated as $s/(n-2)^{1/2}$, where 's' is the standard deviation and 'n' is the sample number of parameters. The asterisk denotes the correlation is significant above the 95% confidence level [Colour figure can be viewed at wileyonlinelibrary.com]

When the AOD ranges from 0.06 to 0.36, the CDNC increases rapidly from 0.07 mm^{-3} to 0.13 mm^{-3}. Furthermore, as shown in Figure 8b, as the AOD varies from 0.06 to 0.19, the CEDR increases very rapidly and reaches its peak of 4.67 μm. Then, when the AOD is larger than 0.19, the CEDR decreases instead of increase continuously. The relation between the precipitation and AOD is similar, in which the precipitation reaches the first peak when the AOD is 0.21. Such variation of cloud properties and precipitation with the increase of AOD is an important manifestation of the saturation effect, which has been well comprehended by previous aerosol-cloud-precipitation interaction studies (Koren *et al.*, 2014; Wang *et al.*, 2015; Guo *et al.*, 2016, 2017). Serving as cloud condensation or ice nuclei, at the beginning, the aerosol particles are activated as cloud nuclei and participated in the cloud. As the cloud condensation nuclei or ice nuclei become saturated, the continued increase of aerosols will cause a decrease in the mean size of cloud droplets under a limited water vapour condition (Twomey, 1977; Rosenfeld and Lensky, 1998; Tao *et al.*, 2012; Wang *et al.*, 2018; Liu *et al.*, 2019a). With the occurrence of saturation effect, the collision-coalescence process is thus inhibited, resulting in longer cloud lifetimes and less precipitation reaching the surface (Albrecht, 1989).

Furthermore, the relationships between the CWP, CDNC, CEDR, precipitation and AOD in the AR and SR of EA were analysed in detail. Over the drylands of EA, the AOD ranges between 0.06–0.50 (Figure 9a) and 0.04–0.33 (Figure 9b), respectively. Similarly, in the following, we performed the analysis for the AOD bins with a sample weight exceeding 1%. As shown in Figure 9c, over the AR of EA, the CWP is strongly dependent on AOD and the linear slope between CWP and AOD is about 6.16 $g \cdot m^{-2}$. With the AOD increasing from 0.07 to 0.44, the CDNC increases slightly from 0.07 mm^{-3} to 0.11 mm^{-3}, showing a weak dependence on the AOD. When the AOD equals 0.21 over the AR of EA, the CDNC reaches the minimum of 0.08 mm^{-3} (Figure 9c) and the CEDR reaches the maximum of 4.55 μm (Figure 9e). Besides, the precipitation increases significantly from 7.77 mm to 26.20 mm with the AOD increasing from 0.07 to 0.44. As shown in Figure 9d, the aerosols exert a more pronounced effect on the CWP

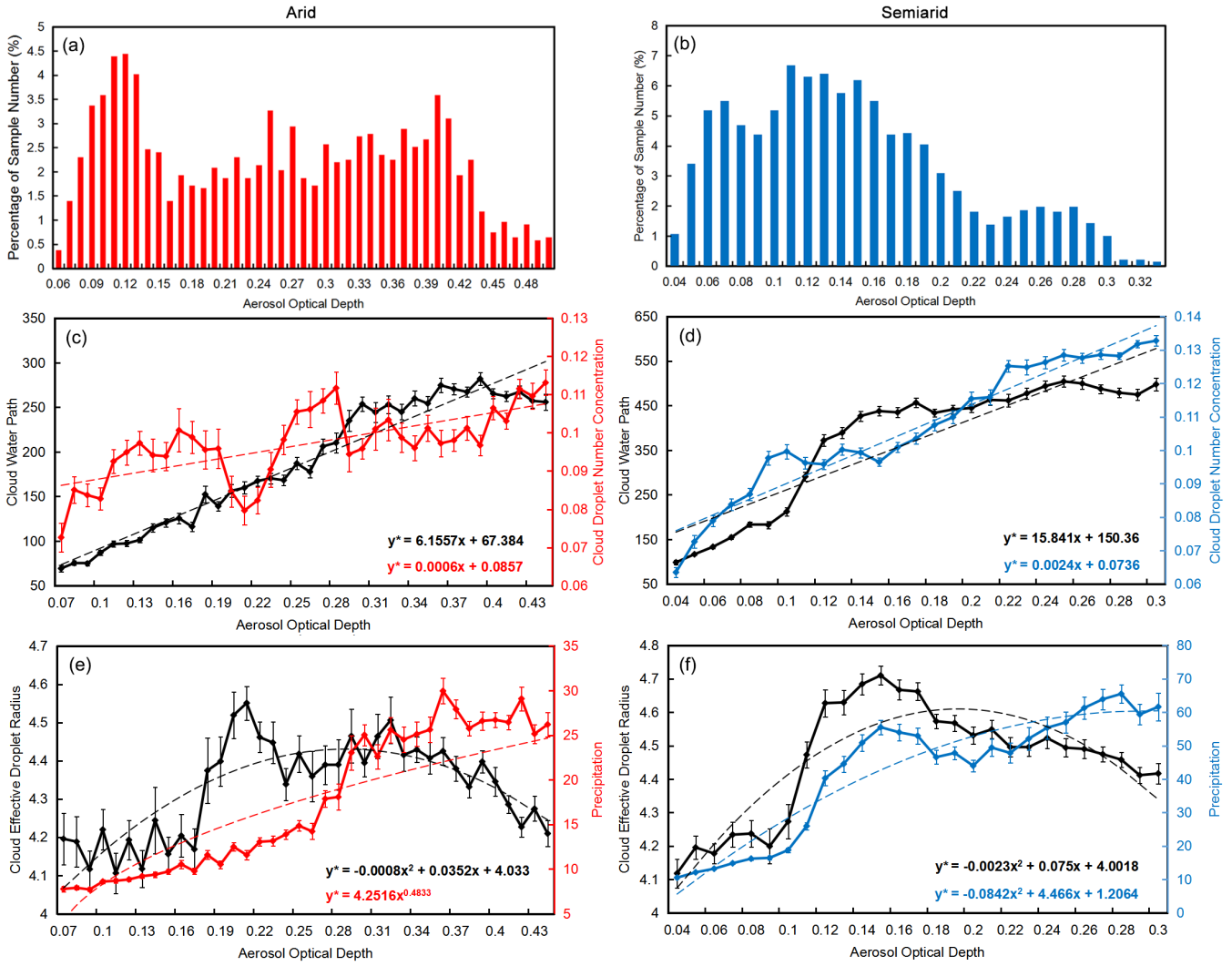

FIGURE 9 Percentage (%) of sample numbers in different AOD bins out of total samples from CMIP5 model results under the 'historical' experiment over the (a) AR and (b) SR of EA during 1850–2005. (c) and (e), (d) and (f) same as in 7a and 7b but for AR and SR of EA, respectively [Colour figure can be viewed at wileyonlinelibrary.com]

and CDNC over the SR than over the AR of EA. Figure 9f shows that, when the AOD ranges from 0.04 to 0.30, the changes in CEDR and precipitation are synchronous over the SR.

Basing on the results of Figure 9, it is suggested that the saturation effect does exist over both drylands except for different threshold values of AOD. Over the SR, for less-to-moderate aerosol loadings (less than 0.15), CWP, CEDR, and precipitation increase rapidly with the increase in AOD. If the aerosol loading is higher, however, the increases in CWP and precipitation with AOD are weakened, even the CEDR begins to decrease. Nevertheless, over the AR, the threshold value of AOD in the saturation effect is 0.21, and the changes in CWP and precipitation are significantly lagged. The different AOD threshold values and the asynchronous changes in CEDR and precipitation may be caused by different meteorological conditions, especially the water vapour condition in the atmosphere over the AR and SR. Also, as reported in previous studies (Yang *et al.*, 2012; Wang *et al.*, 2014; Shi *et al.*, 2017; Jiang *et al.*, 2018; Wang *et al.*, 2018; Liu *et al.*, 2019a), under different meteorological conditions, the responses of clouds and precipitation to aerosol changes are different.

3.3 | Prediction of aerosol, cloud, precipitation and their relationships

Studies have indicated that global drylands have expanded over the last 60 years and will continue to expand in the 21st century, which will pose a severe threat to the ecosystems and inhabitants of drylands (Feng and Fu, 2013; Huang *et al.*, 2016a, 2016b, 2017).

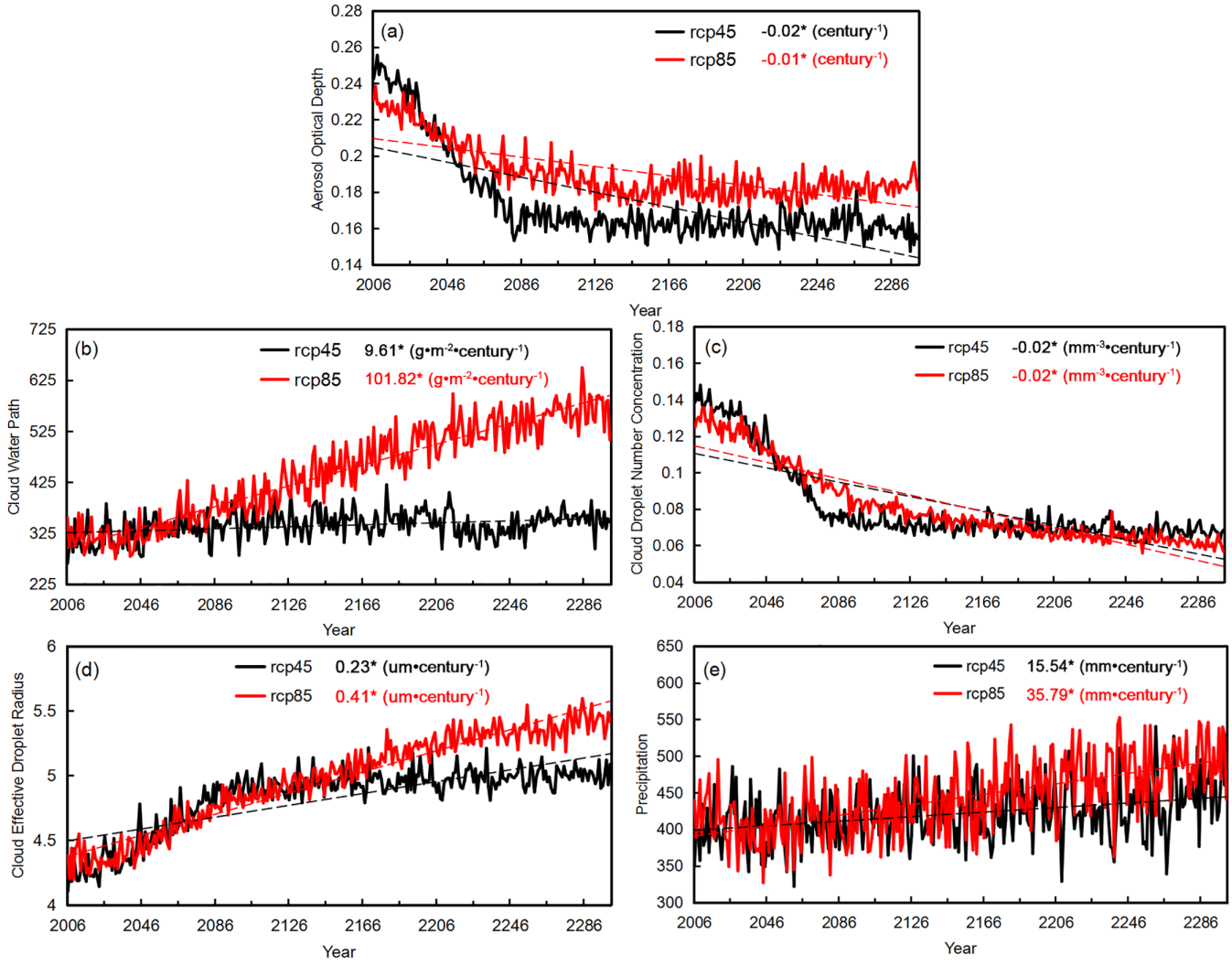

FIGURE 10 Time series of (a) AOD, (b) CWP, (c) CDNC, (d) CEDR, and (e) precipitation simulated by CMIP5 under the 'rcp45' (black line) and 'rcp85' (red line) experiments over the drylands of EA during 2006–2300. The asterisk denotes that the trend is significant above the 95% confidence level [Colour figure can be viewed at wileyonlinelibrary.com]

Therefore, it is urgent to understand the future changes of aerosols, clouds and precipitation and their relationships. Figure 10 presents the time series of annual mean AOD, CWP, CDNC, CEDR and precipitation derived from CMIP5 model results under the 'rcp45' and 'rcp85' experiments over the drylands of EA during 2006–2,300. Overall, except for a more significant decreasing trend of AOD in the 'rcp45' scenario than 'rcp85' scenario, the trends of CWP, CDNC, CEDR and precipitation in the 'rcp85' scenario are more significant than those in the 'rcp45' scenario. As shown in Figure 10a, in the future period from 2006–2,300 under the 'rcp45' and 'rcp85' scenarios, the AODs tend to decrease at rates of −0.02 century^{-1} and -0.01 century^{-1}, respectively, over the drylands of EA. Correspondingly, the CDNC shows a consistent decreasing trend. Besides, the other property parameters including CWP, CEDR and precipitation show a common increasing trend, in which the rising of CWP is much more significant with a rate of 101.82 g·m^{-2}·century^{-1} under the 'rcp85' experiment over the drylands of EA.

Furthermore, in order to analyse the difference between these variables over the AR and SR, here, the time series of annual mean AOD, CWP, CDNC, CEDR and precipitation in the 'rcp85' scenario over the AR and SR of EA are investigated separately. The time series of each variable in the 'rcp85' scenario over the East-Asian AR and SR are shown in Figure 11. Overall, in the 'rcp85' scenario, the changes in these parameters over the SR are more significant than those over the AR during 2006–2,300. Especially, for future projections, a more significant increasing trend of CWP was found over the SR and the rate is 108.38 g·m^{-2}·century^{-1}, while a slightly increasing trend at a rate of

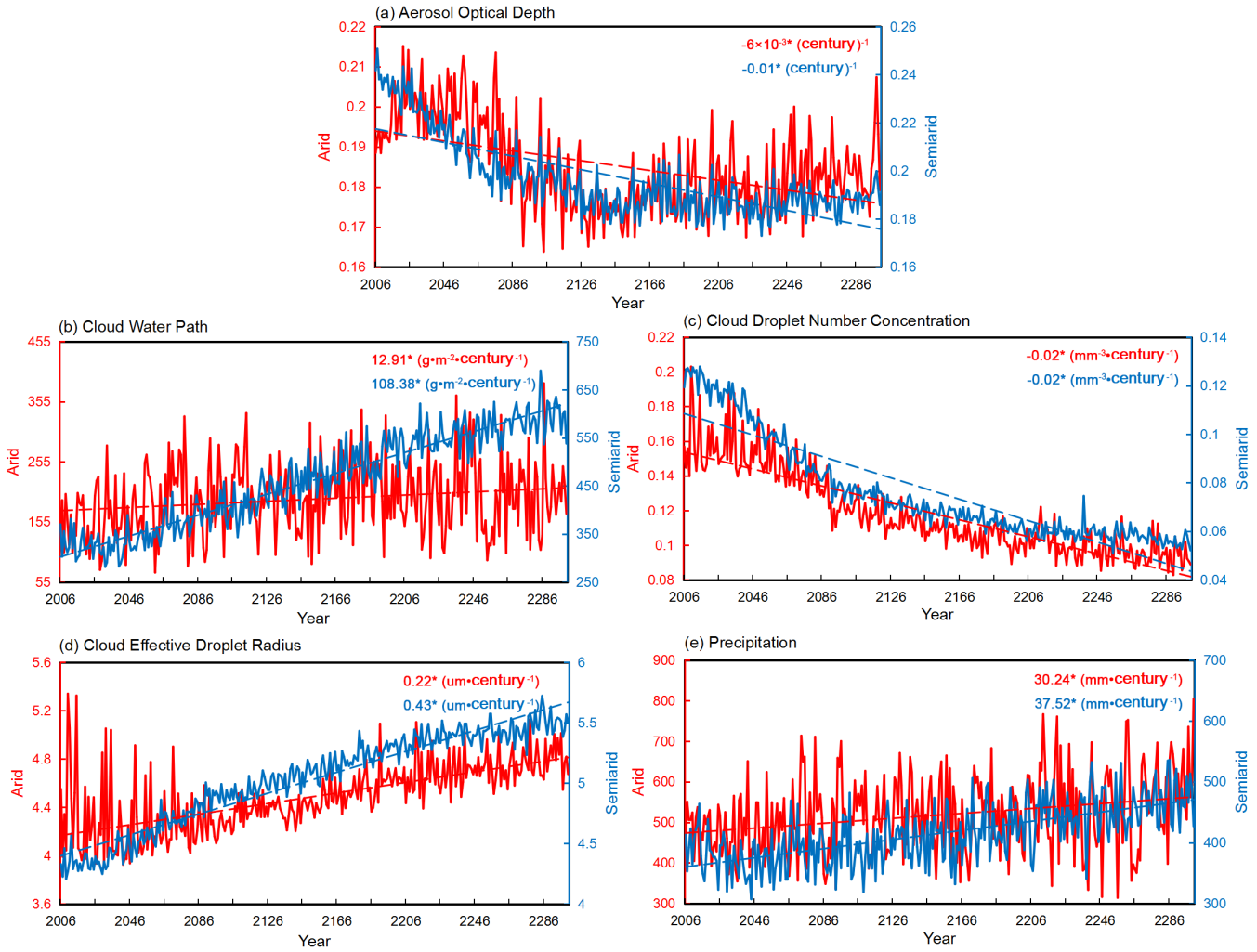

FIGURE 11 Time series of annual mean (a) AOD, (b) CWP, (c) CDNC, (d) CEDR, and (e) precipitation derived from CMIP5 model results under the 'rcp85' scenario over the AR (red line) and SR (blue line) of EA during 2006–2300. The asterisk denotes that the trend is significant above the 95% confidence level [Colour figure can be viewed at wileyonlinelibrary.com]

12.91 g·m^{-2}·century^{-1} was found over the AR in the 'rcp85' scenario.

4 | CONCLUSIONS AND DISCUSSIONS

In this study, the relations between aerosol and cloud, precipitation over the drylands of EA were investigated by CMIP5 models. Based on the historical simulations by CMIP5 models for period 1850–2005, both the AOD and CDNC tend to increase significantly at rates of 0.07 century^{-1} and 0.04 mm^{-3}·century^{-1}, respectively, over the drylands of EA. In addition, the CWP and precipitation show slightly increasing trends (11.52 g·m^{-2}·century^{-1} and 5.80 mm·century^{-1}, respectively), while the CEDR shows a significant decreasing trend over there during the historical period. With the AOD increasing, the CDNC increases significantly, and the CEDR increases first and then decreases. Besides, all of the variables reach the first peak when the AOD equals 0.21 over the drylands of EA. In general, the saturated effect thresholds of aerosol influencing the clouds over the AR and SR of EA are found when the AODs are 0.21 and 0.15, respectively. Furthermore, the results also show that the AOD and CDNC tend to decrease, while the CEDR shows an increasing trend not only under the 'rcp45' but 'rcp85' experiment over the drylands of EA, with significant changes under the 'rcp85' scenario. The CWP and precipitation present slightly increasing trends under the 'historical', 'rcp45' and 'rcp85' scenarios.

Although some valuable findings on the relationship between aerosols, clouds and precipitation over the drylands of EA were gotten, some uncertainties and

limitations introduced by some reasons, such as retrieval uncertainties in aerosol and clouds observations by MODIS, the complexity of the global climate system, the representativeness and reliability of CMIP5 climate models, still remain. In addition, the mechanism relating to aerosol's effects on the clouds and precipitation is very complex. Furthermore, to present the impact of aerosols on atmospheric circulation, we analysed the simulations by these two models under 'sstClimAerosol' and 'sstClim' experiments. We found that the winds (speed and vectors) show an obvious increase due to aerosols over the drylands of EA, especially in the region between 42°N and 50°N. Besides, the vertical velocity difference between the simulations with and without aerosols shows negative values over most regions of AR and SR in EA (except for the SR of northern EA), implying an intensified upward motion in this area. In summary, aerosols have a certain impact on the cloud water path and precipitation in the drylands of EA by affecting circulation (the figures are omitted). Accordingly, more attention should be paid to the aerosol-cloud-precipitation interaction over the drylands in EA by combining observation and improved climate model simulation to adapt the future climate change.

ACKNOWLEDGEMENTS

This research was mainly supported by the National Natural Science Foundation of China (41991231, 91744311, 41521004, and 91937302), Strategic Priority Research Program of the Chinese Academy of Sciences (Grant No. XDA2006010301), and jointly supported by the Fundamental Research Funds for the Central Universities (lzujbky-2020-kb02). We acknowledge the CMIP5 modelling groups for providing accessible simulations, which can be obtained from the website: (https://esgf-node.llnl.gov/search/cmip5/). Click this link to select the 'historical', 'historicalMisc', 'rcp45' and 'rcp85' experiments, 'CSIRO-Mk3-6-0' and 'IPSL-CM5A-LR' models, and 'od550aer', 'clwvi', 'cldncl', 'reffclwtop', and 'pr' variables to download the data. We are also grateful to MODIS teams for providing aerosol and clouds datasets (https://ladsweb.modaps.eosdis.nasa.gov/search/order/4/MOD08_M3–61/2000-01-01..2005-12-31/DNB/World), and CRU teams for providing precipitation (http://data.ceda.ac.uk/badc/cru/data/cru_ts/cru_ts_3.24/data/pre) and potential evapotranspiration (http://data.ceda.ac.uk/badc/cru/data/cru_ts/cru_ts_3.24/data/pet) datasets.

ORCID

Yuzhi Liu https://orcid.org/0000-0001-8310-6975
Tianbin Shao https://orcid.org/0000-0001-9495-9180

REFERENCES

Albrecht, B. (1989) Aerosols, cloud microphysics, and fractional cloudiness. *Science*, 245, 1227–1230. https://doi.org/10.1126/science.245.4923.1227.

Andreae, M.O. (1995) Climatic effects of changing atmospheric aerosol levels. *World Survey of Climatology*, 16(06), 347–398. https://doi.org/10.1016/S0168-6321(06)80033-7.

Andreae, M.O. and Rosenfeld, D. (2008) Aerosol-cloud-precipitation interactions. Part 1. The nature and sources of cloud-active aerosols. *Earth Science Reviews*, 89(1–2), 13–41. https://doi.org/10.1016/j.earscirev.2008.03.001.

Bao, S., Letu, H., Zhao, J., Lei, Y., Zhao, C., Li, J., Tana, G., Liu, C., Guo, E., Zhang, J., He, J. and Bao, Y. (2020) Spatiotemporal distributions of cloud radiative forcing and response to cloud parameters over the Mongolian Plateau during 2003–2017. *International Journal of Climatology*, 40, 4082–4101. https://doi.org/10.1002/joc.6444.

Charlson, R.J. and Heintzenberg, J. (1995) *Aerosol Forcing of Climate*. Chichester, NY: Wiley, p. 416.

Fan, J., Leung, R., Li, Z., Morrison, H., Chen, H., Zhou, Y., Qian, Y. and Wang, Y. (2012) Aerosol impacts on clouds and precipitation in eastern China: results from bin and bulk microphysics. *Journal of Geophysical Research: Atmospheres*, 117, D00K36. https://doi.org/10.1029/2011jd016537.

Fan, J., Rosenfeld, D., Yang, Y., Zhao, C., Leung, L.R. and Li, Z. (2015) Substantial contribution of anthropogenic air pollution to catastrophic floods in southwest China. *Geophysical Research Letters*, 42, 6066–6075. https://doi.org/10.1002/2015GL064479.

Fan, J., Wang, Y., Rosenfeld, D. and Liu, X. (2016) Review of aerosol-cloud interactions: mechanisms, significance and challenges. *Journal of the Atmospheric Sciences*, 73, 4221–4252. https://doi.org/10.1175/JAS-D-16-0037.1.

Feng, S. and Fu, Q. (2013) Expansion of global drylands under a warming climate. *Atmospheric Chemistry and Physics*, 13(19), 10081–10094. https://doi.org/10.5194/acp-13-10081-2013.

Fu, Q., Thorsen, T.J., Su, J., Ge, J. and Huang, J. (2009) Test of Mie-based single-scattering properties of non-spherical dust aerosols in radiative flux calculations. *Journal of Quantitative Spectroscopy and Radiative Transfer*, 110(14–16), 1640–1653. https://doi.org/10.1016/j.jqsrt.2009.03.010.

Guan, X., Huang, J., Guo, R. and Lin, P. (2015) The role of dynamically induced variability in the recent warming trend slowdown over the northern hemisphere. *Scientific Reports*, 5, 12669. https://doi.org/10.1038/srep12669.

Guo, J., Deng, M., Lee, S.S., Wang, F., Li, Z., Zhai, P., Liu, H., Lv, W., Yao, W. and Li, X. (2016) Delaying precipitation and lightning by air pollution over the Pearl River Delta. Part I: Observational analyses. *Journal of Geophysical Research*, 121, 6472–6488. https://doi.org/10.1002/2015JD023257.

Guo, J., Su, T., Li, Z., Miao, Y., Li, J., Liu, H., Xu, H., Cribb, M. and Zhai, P. (2017) Declining frequency of summertime local-scale precipitation over eastern China from 1970 to 2010 and its potential link to aerosols. *Geophysical Research Letters*, 44, 5700–5708. https://doi.org/10.1002/2017GL073533.

Houghton, J.T., Ding, Y. and Griggs, D.J. (2001) *Climate change: the scientific basis*. New York, NY: Cambridge University Press, pp. 1–421.

Hua, S., Liu, Y., Luo, R., Shao, T. and Zhu, Q. (2020) Inconsistent aerosol indirect effects on water clouds and ice clouds over the

Tibetan Plateau. *International Journal of Climatology*, 40, 1–17. https://doi.org/10.1002/joc.6430.

Huang, J., Guan, X. and Ji, F. (2012) Enhanced cold-season warming in semi-arid regions. *Atmospheric Chemistry and Physics*, 12, 5391–5398. https://doi.org/10.5194/acp-12-5391-2012.

Huang, J., Huang, J.P., Liu, X., Li, C., Ding, L. and Yu, H. (2018) The global oxygen budget and its future projection. *Science Bulletin*, 63, 1180–1186. https://doi.org/10.1016/j.scib.2018.07.023.

Huang, J., Ji, M., Liu, Y. and Zhang, L. (2013) An overview of arid and semi-arid climate change. *Advances in Climate Change Research*, 9, 9–14. https://doi.org/10.3969/j.issn.1673-1719.2013.01.002.

Huang, J., Ji, M., Xie, Y., Wang, S., He, Y. and Ran, J. (2016a) Global semi-arid climate change over last 60 years. *Climate Dynamics*, 46(3–4), 1131–1150. https://doi.org/10.1007/s00382-015-2636-8.

Huang, J., Li, Y., Fu, C., Chen, F., Fu, Q. and Dai, A. (2017) Dryland climate change: recent progress and challenges. *Reviews of Geophysics*, 55, 719–778. https://doi.org/10.1002/2016RG000550.

Huang, J., Lin, B., Minnis, P., Wang, T.H., Wang, X., Hu, Y.X., Yi, Y.H. and Ayerse, J.K. (2006) Satellite-based assessment of possible dust aerosols semi-direct effect on cloud water path over East Asia. *Geophysical Research Letters*, 33, L19802. https://doi.org/10.1029/2006GL026561.

Huang, J., Wang, T., Wang, W., Li, Z. and Yan, H. (2014) Climate effects of dust aerosols over East Asian arid and semiarid regions: climate effects of East Asian dust. *Journal of Geophysical Research: Atmospheres*, 119, 113989–111416. https://doi.org/10.1002/2014JD021796.

Huang, J., Yu, H., Guan, X., Wang, G. and Guo, R. (2016b) Accelerated dryland expansion under climate change. *Nature Climate Change*, 6(2), 166–171. https://doi.org/10.1038/nclimate2837.

Huang, J., Zhang, W., Zuo, J., Bi, J., Shi, J., Wang, X., Chang, Z., Huang, Z., Yang, S., Zhang, B., Wang, G., Feng, G., Yuan, J., Zhang, L., Zuo, H., Wang, S., Fu, C. and Chou, J. (2008) An overview of the semi-arid climate and environment research observatory over the Loess Plateau. *Advances in Atmospheric Sciences*, 25(6), 1–16. https://doi.org/10.1007/s00376-008-0906-7.

IPCC. (2007) *Climate change 2007: the physical science basis*. Summary for Policymakers.

Jia, R., Liu, Y., Hua, S., Zhu, Q. and Shao, T. (2018) Estimation of the aerosol radiative effect over the Tibetan Plateau based on the latest CALIPSO product. *Journal of Meteorological Research*, 32(5), 707–722. https://doi.org/10.1007/s13351-018-8060-3.

Jiang, J., Su, H., Huang, L., Wang, Y., Massie, S., Zhao, B., Omar, A. and Wang, Z. (2018) Contrasting effects on deep convective clouds by different types of aerosols. *Nature Communications*, 9, 3874. https://doi.org/10.1038/s41467-018-06280-4.

Jiang, M., Li, Z., Wan, B. and Cribb, M.C. (2016) Impact of aerosols on precipitation from deep convective clouds in eastern China. *Journal of Geophysical Research: Atmospheres*, 121, 9607–9620. https://doi.org/10.1002/2015JD024246.

Jiang, Y., Liu, X., Yang, X.Q. and Wang, M. (2013) A numerical study of the effect of different aerosol types on East Asian summer clouds and precipitation. *Atmospheric Environment*, 70, 51–63. https://doi.org/10.1016/j.atmosenv.2012.12.039.

Jiang, Y., Yang, X.Q., Liu, X., Yang, D., Sun, X., Wang, M., Ding, A., Wang, T. and Fu, C. (2017) Anthropogenic aerosol effects on East Asian winter monsoon: the role of black carbon-induced Tibetan Plateau warming. *Journal of Geophysical Research: Atmospheres*, 122, 5883–5902. https://doi.org/10.1002/2016JD026237.

Koren, I., Dagan, G. and Altaratz, O. (2014) From aerosol-limited to invigoration of warm convective clouds. *Science*, 344(6188), 1143–1146. https://doi.org/10.1126/science.1252595.

Lee, S.S. (2012) Effect of aerosol on circulations and precipitation in deep convective clouds. *Journal of the Atmospheric Sciences*, 69, 1957–1974. http://doi.org/10.1175/jas-d-11-0111.1.

Lee, S.S., Tao, W.-K. and Jung, C.-H. (2015) Aerosol effects on instability, circulations, clouds, and precipitation. *Advances in Meteorology*, 2014, 683950–683958. http://doi.org/10.1155/2014/683950.

Li, G., Wang, Y. and Zhang, R. (2008) Implementation of a two-moment bulk microphysics scheme to the WRF model to investigate aerosol-cloud interaction. *Journal of Geophysical Research*, 113, D15211. https://doi.org/10.1029/2007JD009361.

Li, Z., Niu, F., Fan, J., Liu, Y., Rosenfeld, D. and Ding, Y. (2011) Long-term impacts of aerosols on the vertical development of clouds and precipitation. *Nature Geoscience*, 4, 888–894. http://doi.org/10.1038/ngeo1313.

Li, Z., Rosenfeld, D. and Fan, J. (2017) Aerosols and their impact on radiation, clouds, precipitation, and severe weather events. *Oxford Research Encyclopedia of Environmental Science*. Oxford University Press USA, 1–36. https://doi.org/10.1093/acrefore/9780199389414.013.126.

Li, Z., Wang, Y., Guo, J., Zhao, C., Cribb, M.C., Dong, X., Fan, J., Gong, D., Huang, J., Jiang, M., Jang, Y., Lee, S.S., Li, H., Li, J., Liu, J., Qian, Y., Rosenfeld, D., Shan, S., Sun, Y., Wang, H., Xin, J., Yan, X., Yang, X., Zhang, F. and Zheng, Y. (2019) East asian study of tropospheric aerosols and their impact on regional clouds, precipitation, and climate (EAST-AIR$_{CPC}$). *Journal of Geophysical Research: Atmospheres*, 124(13), 26–54. https://doi.org/10.1029/2019JD030758.

Liu, Y., Hua, S., Jia, R. and Huang, J. (2019a) Effect of aerosols on the ice cloud properties over the Tibetan Plateau. *Journal of Geophysical Research: Atmospheres*, 124, 9594–9608. https://doi.org/10.1029/2019JD030463.

Liu, Y., Li, Y., Huang, J., Zhu, Q. and Wang, S. (2020a) Attribution of the Tibetan Plateau to northern drought. *National Science Review*, 7(3), 489–492. https://doi.org/10.1093/nsr/nwz191.

Liu, Y., Luo, R., Zhu, Q., Hua, S. and Wang, B. (2019b) Cloud ability to produce precipitation over arid and semiarid regions of Central and East Asia. *International Journal of Climatology*, 40(3), 1824–1837. https://doi.org/10.1002/joc.6304.

Liu, Y., Shao, T., Hua, S., Zhu, Q. and Luo, R. (2020b) Association of anthropogenic aerosols with subtropical drought in East Asia. *International Journal of Climatology*, 40(7), 3500–3513. https://doi.org/10.1002/joc.6410.

Liu, Y., Wu, C., Jia, R. and Huang, J. (2018) An overview of the influence of atmospheric circulation on the climate in arid and semi-arid region of Central and East Asia. *Science China (Earth Sciences)*, 61, 1183–1194. https://doi.org/10.1007/s11430-017-9202-1.

Liu, Y., Zhu, Q., Huang, J., Hua, S. and Jia, R. (2019c) Impact of dust-polluted convective clouds over the Tibetan Plateau on downstream precipitation. *Atmospheric Environment*, 209, 67–77. https://doi.org/10.1016/j.atmosenv.2019.04.001.

Lohmann, U. and Feichter, J. (2005) Global indirect aerosol effects: a review. *Atmospheric Chemistry and Physics*, 5, 715–737. https://doi.org/10.5194/acp-5-715-2005.

Ma, R., Letu, H., Yang, K., Wang, T., Shi, C., Xu, J., Shi, J., Shi, C. and Chen, L. (2020) Estimation of surface shortwave radiation from Himawari-8 satellite data based on a combination of radiative transfer and deep neural network. *IEEE Transactions on Geoscience and Remote Sensing*, 240, 106672–105316. https://doi.org/10.1109/TGRS.2019.2963262.

Manaster, A., O'Dell, C. and Elsaesser, G. (2017) Evaluation of cloud liquid water path trends using a multidecadal record of passive microwave observations. *Journal of Climate*, 30, 5871–5884. https://doi.org/10.1175/JCLI-D-16-0399.1.

McComiskey, A. and Feingold, G. (2012) The scale problem in quantifying aerosol indirect effects. *Atmospheric Chemistry and Physics*, 12, 1031–1049. https://doi.org/10.5194/acp-12-1031-2012.

Qi, Y., Ge, J. and Huang, J. (2013) Spatial and temporal distribution of MODIS and MISR aerosol optical depth over northern China and comparison with AERONET. *Chinese Science Bulletin*, 58 (20), 2497–2506. http://doi.org/10.1007/s11434-013-5678-5.

Qian, Y., Leung, L.R., Ghan, S.J. and Giorgi, F. (2003) Regional climate effects of aerosols over China: modeling and observation. *Tellus Series B Chemical and Physical Meteorology*, 55, 914–934. http://doi.org/10.1046/j.1435-6935.2003.00070.x.

Reynolds, J.F., Stafford Smith, D.M., Lambin, E.F., Turner, B.L., II, Mortimore, M., Batterburye, S.P.J., Downing, T.E., Dowlatabadi, H., Fernández, R.J., Herrickt, J.E., Huber-Sannwald, E., Jiang, H., Leemans, R., Lynam, T., Maestre, F., Ayarza, M. and Walker, B. (2007) Global desertification: building a science for dryland development. *Science*, 316, 847–851. https://doi.org/10.1126/science.1131634.

Rosenfeld, D., Andreae, M.O., Asmi, A., Chin, M., Leeuw, G., Donovan, D.P., Kahn, R., Kinne, S., Kivekas, N., Kulmala, M., Lau, W., Schmidt, S., Suni, T., Wagner, T., Wild, M. and Quaas, J. (2014) Global observations of aerosol-cloud-precipitation climate interactions. *Reviews of Geophysics*, 52, 750–808. http://doi.org/10.1002/2013rg000441.

Rosenfeld, D. and Lensky, I.M. (1998) Satellite-based insights into precipitation formation processes in continental and maritime convective clouds. *Bulletin of the American Meteorological Society*, 79, 2457–2476. https://doi.org/10.1175/1520-0477(1998)079<2457:SBIIPF>2.0.CO;2.

Ryan, C. and Elsner, P. (2016) The potential for sand dams to increase the adaptive capacity of East African drylands to climate change. *Regional Environment Change*, 16, 2087–2096. https://doi.org/10.1007/s10113-016-0938-y.

Sato, T. (2007) Water sources in semiarid northeast Asia as revealed by field observations and isotope transport model. *Journal of Geophysical Research: Atmospheres*, 112, D17112. https://doi.org/10.1029/2006JD008321.

Shi, L., Zhang, J., Yao, F., Han, X., Igbawua, T., Liu, Y. and Zhang, D. (2017) Influence of meteorological conditions on correlation between aerosol and cloud in summer. *Advances in Space Research*, 59(7), 1907–1920. https://doi.org/10.1016/j.asr.2017.01.026.

Soden, B. and Held, I. (2006) An assessment of climate feedbacks in coupled ocean-atmosphere models. *Journal of Climate*, 19, 3354–3360. https://doi.org/10.1175/JCLI3799.1.

Stjern, C.W. and Kristjánsson, J.E. (2015) Contrasting influences of recent aerosol changes on clouds and precipitation in Europe and East Asia. *Journal of Climate*, 28(22), 8770–8790. http://doi.org/10.1175/jcli-d-14-00837.1.

Tao, W.K., Chen, J.P., Li, Z., Wang, C. and Zhang, C. (2012) Impact of aerosols on convective clouds and precipitation. *Reviews of Geophysics*, 50, RG2001. https://doi.org/10.1029/2011RG000369.

Taylor, K.E., Stouffer, R.J. and Meehl, G.A. (2012) An overview of CMIP5 and the experiment design. *Bulletin of the American Meteorological Society*, 93(4), 485–498. https://doi.org/10.1175/BAMS-D-11-00094.1.

Twomey, S. (1977) The influence of pollution on the shortwave albedo of clouds. *Journal of the Atmospheric Sciences*, 34(7), 1149–1152. https://doi.org/10.1175/1520-0469(1977)034<1149:TIOPOT>2.0.CO;2.

Vallejo, V., Smanis, A., Chirino, E., Fuentes, D., Valdecantos, A. and Vilagrosa, A. (2012) Perspectives in dryland restoration: approaches for climate change adaptation. *New Forests*, 43, 561–579. https://doi.org/10.1007/s11056-012-9325-9.

Wang, F., Guo, J., Zhang, J., Huang, J., Min, M., Chen, T., Liu, H., Deng, M. and Li, X. (2015) Multi-sensor quantification of aerosol-induced variability in warm cloud properties over eastern China. *Atmospheric Environment*, 113, 1–9. https://doi.org/10.1016/j.atmosenv.2015.04.063.

Wang, Q., Li, Z., Guo, J., Zhao, C. and Cribb, M. (2018) The climate impact of aerosols on the lightning flash rate: is it detectable from long-term measurements? *Atmospheric Chemistry and Physics*, 18(12), 797–816. https://doi.org/10.5194/acp-18-12797-2018.

Wang, S., He, W., Chen, H., Bian, J. and Wang, Z. (2010) Statistics of cloud height over the Tibetan Plateau and its surrounding region derived from the CloudSat data. *Plateau Meteorology*, 29, 1–9. https://doi.org/10.3788/gzxb20103906.0998.

Wang, W., Huang, J., Zhou, T., Bi, J., Lin, L., Chen, Y., Huang, Z. and Su, J. (2013) Estimation of radiative effect of a heavy dust storm over northwest China using Fu-Liou model and ground measurements. *Journal of Quantitative Spectroscopy and Radiative Transfer*, 122, 114–126. https://doi.org/10.1016/j.jqsrt.2012.10.018.

Wang, Y., Wan, Q., Meng, W., Liao, F., Tan, H. and Zhang, R. (2011) Long-term impacts of aerosols on precipitation and lightning over the Pearl River Delta megacity area in China. *Atmospheric Chemistry and Physics*, 11(12), 421–436. https://doi.org/10.5194/acp-11-12421-2011.

Wang, Y., Zhang, J., Wang, L., Hu, B., Tang, G., Liu, Z., Sun, Y. and Ji, D. (2014) Researching significance, status and expectation of Haze in Beijing Tianjin Heibei Region. *Advances in Earth Science*, 29(3), 388–396. https://doi.org/10.11867/j.issn.1001-8116.2014.03.0388.

Wang, Y.H. and Chen, W. (2012) Interannual variations of summer rainfall and their causes in the mid-latitude arid/semi-arid areas of East Asia. *Climatic and Environmental Research*, 17, 444–456. https://doi.org/10.1007/s11783-011-0280-z.

Yan, H., Qian, Y., Zhao, C., Wang, H., Wang, M., Yang, B. and Fu, Q. (2015) A new approach to modeling aerosol effects on East Asian climate: parametric uncertainties associated with emissions, cloud microphysics, and their interactions. *Journal of Geophysical Research: Atmospheres*, 120, 8905–8924. https://doi.org/10.1002/2015JD023442.

Yang, X., Ferrat, M. and Li, Z. (2012) New evidence of orographic precipitation suppression by aerosols in central China. *Meteorology and Atmospheric Physics*, 119(1–2), 17–29. https://doi.org/10.1007/s00703-012-0221-9.

Zhang, D., Liu, D., Luo, T., Wang, Z. and Yin, Y. (2015) Aerosol impacts on cloud thermodynamic phase change over East Asia observed with CALIPSO and CloudSat measurements. *Journal of Geophysical Research: Atmospheres*, 120, 1490–1501. http://doi.org/10.1002/2014JD022630.

Zhao, C., Tie, X. and Lin, Y. (2006) A possible positive feedback of reduction of precipitation and increase in aerosols over eastern central China. *Geophysical Research Letters*, 33, L11814. https://doi.org/10.1029/2006GL025959.

How to cite this article: Luo R, Liu Y, Zhu Q, Tang Y, Shao T. Effects of aerosols on cloud and precipitation in East-Asian drylands. *Int J Climatol*. 2021;41:4603–4618. https://doi.org/10.1002/joc.7089